PROCEEDINGS OF SPIE

SPIEDigitalLibrary.org/conference-proceedings-of-spie

Bowtie plasmonic nanoantenna arrays for polarimetric optical biosensing

Jonathan Calderón, Jesús Álvarez, Juan Martinez-Pastor, Daniel Hill

Jonathan Calderón, Jesús Álvarez, Juan Martinez-Pastor, Daniel Hill, "Bowtie plasmonic nanoantenna arrays for polarimetric optical biosensing," Proc. SPIE 8933, Frontiers in Biological Detection: From Nanosensors to Systems VI, 89330I (5 March 2014); doi: 10.1117/12.2039644

SPIE.

Event: SPIE BiOS, 2014, San Francisco, California, United States

Bowtie plasmonic nanoantenna arrays for polarimetric optical biosensing

Jonathan Calderón, Jesús Álvarez. Juan Martínez-Pastor, Daniel Hill
Unit of Optoelectronic Materials and Devices, Materials Science Institute, University of Valencia, P.O. Box 22085, 46071 Valencia, Spain

ABSTRACT

We report on the first polarimetric plasmonic biosensor based on arrays of bowtie nanoantennas. Using the Finite Element Method (FEM) the phase retardation between the components of light polarized parallel and perpendicular to the axis of the nanoantennas is studied. After optimizing them for high volumetric sensitivity at a wavelength of 780 nm, sensitivities ~5 rad/RIU are obtained, corresponding to a detection limit ~10^{-7} RIU when using the polarimetric readout platform. Surface sensitivity values resulted from studies of phase retardation changes from a coverage of bioreceptors and analytes.

Keywords: gold bowties, nanoantenna arrays, polarimetry, surface plasmon polaritons, optical sensing and biosensing, LSPR, FEM simulations, phase retardation.

1. INTRODUCTION

Plasmonic nanostructures are metallic materials patterned at the nanoscale that exhibit interesting optical properties due to the large enhancement and localization of the electromagnetic fields. The interaction between metallic patterns and light leads to a collective oscillations of the electronic charge density localized at the metal surface, called Localized Surface Plasmon Resonance (LSPR). The energy of these plasmons depends on the size, geometry and composition of the nanostructures as well as on the dielectric environment that surrounds them, subsequently many such structures have been engineered to provide diverse functions such as SERS [1], nanotweezing [2, 3] or, as we report here, biosensing [4, 5]. When two nanoparticles are close enough for strong coupling to take place between them, electromagnetic fields of several times that of the incident light arise in their gap [6]. Subsequent refractive index variations in the gap result in significantly greater displacements of resonance peaks compared to non-coupled metal nanostructures. Moreover, array structures can induce collective plasmons that can improve this sensitivity further still [7, 8].

In photonic biosensing, measurements of the signal phase when sensitive to refractive index variations in the sensor, through a combination of phase modulation of the light source and a post-measurement Fast Fourier Transform or in-situ phase locked loop measurement result in considerably lower noise compared to intensity measurements [9, 10]. Furthermore measurements of the phase difference between two orthogonally polarized waves after their interaction with a nanoantenna is independent of intensity, provided the signal is distinguished from the noise. Consequently, although most plasmonic nanoantenna biosensing research reported has been done with intensity measurements LSPR phase measurement sensing has been shown to improve the sensitivity over that from intensity-based measurements [11]. In this paper we explore an alternative scheme for LSPR phase measurement based biosensing by exploiting the symmetry breaking induced by the geometry of a bowtie nanoantenna (Fig. 1). Specifically, the lack of axial symmetry of these nanoantennas results in normally incident light polarized along and perpendicular to the major axis of the bowtie experiencing different phase retardation upon scattering, whose difference will be strongly dependent on the refractive index changes of the surroundings.

Frontiers in Biological Detection: From Nanosensors to Systems VI,
edited by Benjamin L. Miller, Philippe M. Fauchet, Brian T. Cunningham, Proc. of SPIE
Vol. 8933, 89330I · © 2014 SPIE · CCC code: 1605-7422/14/$18 · doi: 10.1117/12.2039644

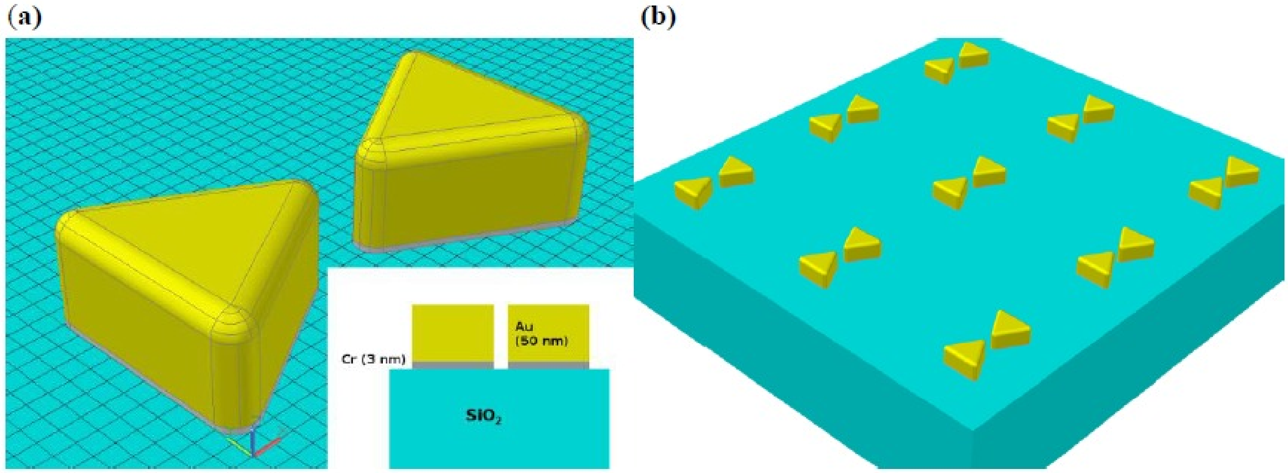

Figure 1: Schematic views of the gold bowtie nanoantenna (a) and the gold bowtie nanoantenna array (b).

2. METHODOLOGY

The finite element method (FEM) was used to calculate the LSPR characteristics of gold bowtie nanoantennas, in order to investigate their sensing capabilities. This method allows us to obtain a numerical solution for a structure (in which a set of partial differential equations that characterize its physical behavior has been defined) by discretizing it into a set of subdomains called "finite elements". The refractive index of the substrate (silica) was taken to be 1.51 and the refractive index of the surrounding aqueous media is 1.33 in all simulations. The real and imaginary refractive indices of the chosen plasmonic material, gold, are modeled through an interpolation with splines of the experimental data obtained by Palik *et al.* [12]. The bowtie nanoantennas were then drawn with a radius of curvature on their tips of 15 nm, so as to avoid divergences induced by extremely spiky tips and to better approximate fabricated nanoantennas [13]. Thereafter a linearly polarized electromagnetic plane wave was sent from the surrounding media under normal incidence. A sweep for different wavelengths is performed in order to obtain the plasmonic spectra.

The modeling was done using COMSOL [14], a commercial software based on the FEM; a scattering mode with a background field was introduced as an analytic expression. In the model, two semi-infinite media (water and silica) are used so the background field is defined as the sum of the incident and reflected wave in the first media and the transmitted wave in the second media through the use of the Fresnel equations. For the simulation of an isolated nanoantenna, we have placed PMLs (Perfect Matched Layers, which are domains with the same refractive index as the surrounding domains at their boundary but with increasing imaginary refractive index when moving away from it) and SBC (Scattering Boundary Conditions, boundaries transparent for scattered waves) around the entire physical domain. These boundary conditions result in an absorption of the EM waves that arrive at the boundaries of our physical domain, preventing unphysical reflections. In order to account for the double-periodic nature of the array simulation, PMLs and SBCs were also placed at the top and the bottom of the unit cell and PECs (Perfect Electric Conditions, which nullify the electric field component perpendicular to the boundary surface) and PMCs (Perfect Magnetic Conditions, which nullify the magnetic field component perpendicular to the boundary surface) on its side walls. The PECs were placed on the two walls perpendicular to the polarization of the normal incident wave and the PMCs on the others, making the side walls act like mirrors, with the effect of a periodic array being obtained [15]. The separation of nanoantennas was equalized to that of the unit cell size.

3. RESULTS AND DISCUSSION

3.1 Isolated bowties

The localized plasmonic near-field of the bowtie nanoantennas, which is very sensitive to the refractive index of its surrounding medium can be tuned by modifying the nanostructure shape. Geometrical parameters such as size, gap distance [16], height [17], bowtie angle [18, 19] and sharpness of the tips [15, 20] have a direct influence in the LSPR, changing the spectral position and narrowness of the plasmonic peak in the extinction cross-section. Taking into account the fabrication limitations and aiming for a LSPR peak wavelength around 780 nm, which is a standard wavelength of near IR diode lasers used in Surface Enhanced Raman Scattering (SERS), we fixed the height of the nanoparticles to 50 nm, the length of their sides to 120 nm and the curvature of the vertices to a 15 nm sphere radius. The nanoparticles were modeled as equilateral triangles and a chrome adhesion layer of 3 nm of thickness was added under the gold nanoparticles, as can be observed in Fig. 1a, which is needed in actual applications for the gold to adhere to the SiO_2 substrate. The presence of a metal adhesion layer induces the broadening of the LSPR and diminishes the scattering amplitude [21] and therefore the adhesion layer should be maintained as thin as possible. The choice of the substrate is very important due to the screening effect [22] and so it is convenient to choose a substrate with a refractive index as close as possible to that of the medium that surrounds the bowties.

As expected, an incident linearly polarized wave with electric field parallel to the major axis of the bowtie results in a high confinement of electric field within the gap region of the nanoantenna [Fig. 2a], with enhancement factors (|E|/|E0|) up to a factor 100 for the smallest gap simulated (5 nm). However, if the polarization is perpendicular, the enhancement regions are located around the other tips of the bowtie [Fig. 2b], far from the gap region, and the enhancement factor becomes considerably lower.

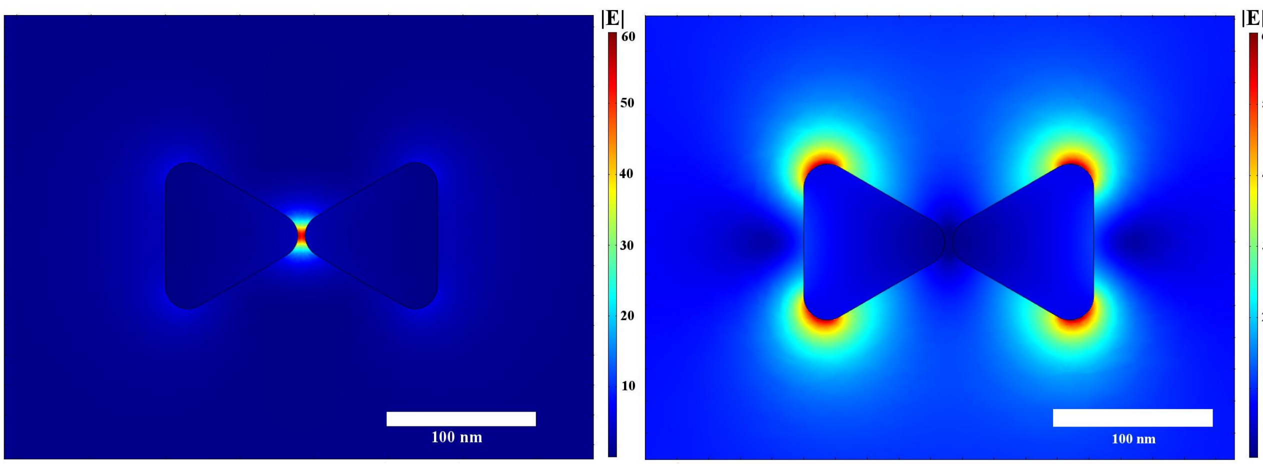

Figure 2: Electric field distribution at the LSPR frequency for incident light polarized along (a) and perpendicular (b) to the major axis of a bowtie nanoantenna with a gap of 5 nm

We then carried out simulations for various gap lengths, calculating the extinction spectra for both polarization directions in order to study the plasmon peak width and shift [Fig. 3a]. Along the direction parallel to the major axis of the bowtie an increasing redshift of the more intense and lower energy plasmon resonance is observed by narrowing the gap, contrary to the perpendicular case with its shorter wavelength plasmon resonance, where the redshift is practically absent. These resonant plasmonic modes at short and long wavelengths are characteristics of the single particle and dimmer of the bowtie, respectively, and their calculated extinction cross-section is consistent with extinction efficiency and transmission data for similar nanoparticles modelled elsewhere [16]. Actually, as the length of the gap increases the extinction spectra of the perpendicular and parallel excitations converge, this fact and the absence of a significant redshift in the perpendicular mode can both be explained by the separation of field enhancement locations: direct dipolar coupling (which is a near-field effect that decreases as $\sim 1/r^3$)) between the two particles is very weak.

The phase of the scattered wave is calculated as

$$\varphi_i = \arctan\left(\frac{\operatorname{Im}\{E_i\}}{\operatorname{Re}\{E_i\}}\right) \tag{1}$$

for both polarizations and the phase difference between them is determined by

$$\Delta_{\varphi} = \varphi_x^{\parallel} - \varphi_y^{\perp} \tag{2}$$

according to the electric field components that dominate in both polarization modes. Characteristic spectra were then obtained for each gap distance [Fig. 3b] and once again two plasmon resonances are observed. The one at a longer wavelength is that associated with the polarization along the major axis of the bowtie system, for which a noticeable redshift and broadening is observed, as it is also in the extinction spectra.

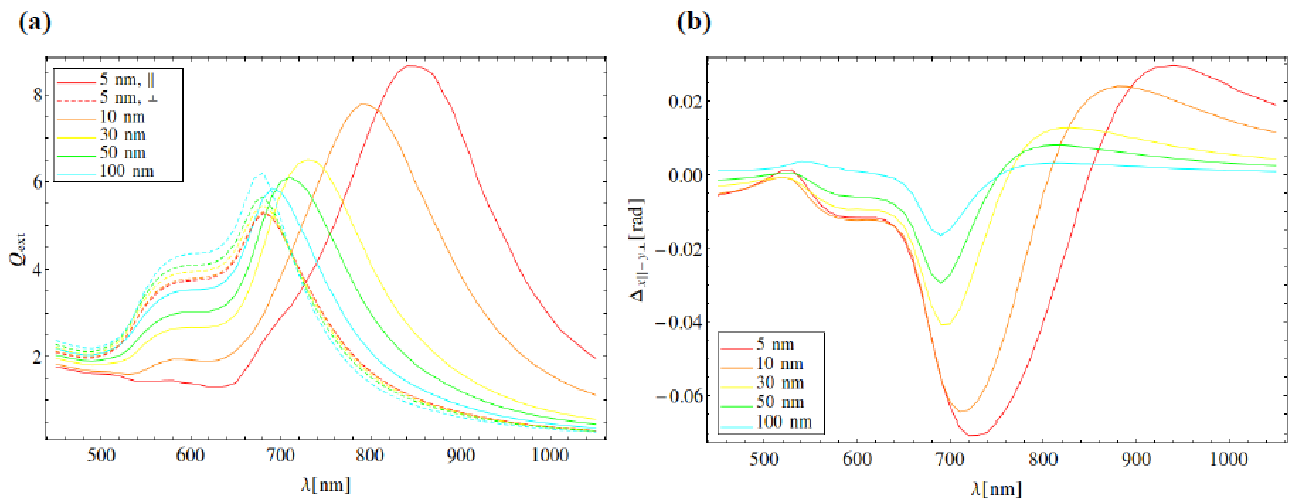

Figure 3: (a). Extinction spectra of the bowtie nanoantenna for polarization parallel (continuous lines) and perpendicular (dashed lines) to the major axis of the bowtie for different gaps (b) Phase difference spectra for different gaps.

In the subsequent sections a gap of 30 nm was chosen for all simulations so that the bowtie nanoantenna may have a good sensitivity whilst still being feasible for fabrication by technologies suitable for production of commercial biosensors [23].

3.2 Bowtie array

If the wavelength of the scattered light is close to both the pitch distances of the array and the LSPR wavelength then a dramatic modification of the extinction cross-section will arise due to a collective coupling of every localized plasmon. When excited by an EM wave at frequency ω, a dipole radiates a scattered wave proportionally to its dipole moment and so the net field at every dipole is therefore the sum of the incident field plus the radiation of all the others dipoles, which leads to a system of coupled equations. Therefore, by adjusting the pitch distances of the array, a narrowing of the resonance can be achieved through radiative coupling. A model based on the Dipole Array Approximation (DAA) works very well when the nanoparticles of the array are spheres and ellipsoids and can be easily numerically calculated [7, 8, 24]. However, when we consider triangular prisms like the present case, the expression of the polarizabillity becomes extremely complex and numerical simulations based on methods such as FEM, DDA or FDTD are demanded [25].

Once the size, gap and height of the bowties were decided, FEM simulations for different values of vertical and horizontal pitch periods (Dx and Dy) were run, a sample of these simulations can be found in Fig. 4, where can be observed how the lineshape of the LSPR spectra can be tuned by varying the pitch period of the array. The main criterion was to obtain the narrowest plasmonic peak centered at around 780 nm for the parallel mode plasmon, and hence, the best sensitivity in intensity at this wavelength. The optimum pitches were found to be Dx = 525 nm and Dy = 525 nm and so this array was used in all of the sensing simulations reported in the following sections.

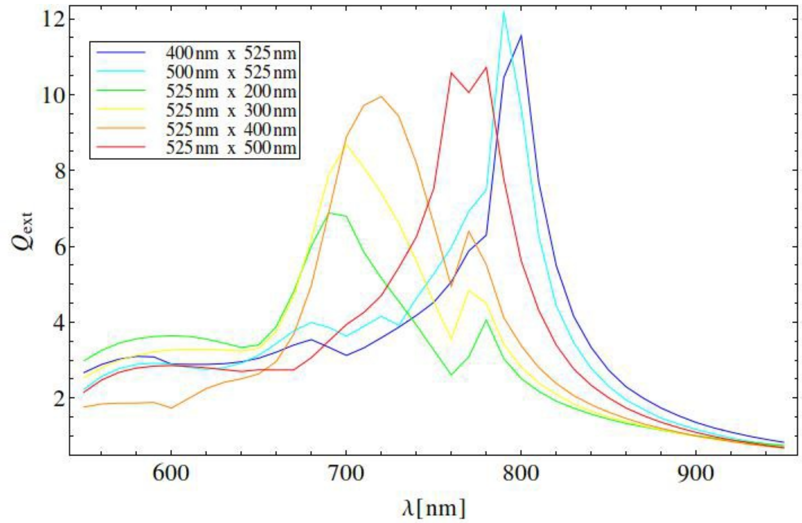

Figure 4: Extinction efficiencies obtained from the simulation of arrays with different pitch periods.

3.2.1 Bulk refractive index sensing

In reflectance and transmittance measurements the intensity signal is proportional to the extinction cross section, and so by studying the variation of the extinction spectra with respect to the refractive index we can obtain the sensitivity and thereafter detection limit of the sensing system based on the phase retardation measurement. We therefore performed simulations for different values of the refractive index of the medium occupying the half space above the bowtie array for both EM field polarizations [Fig. 5].

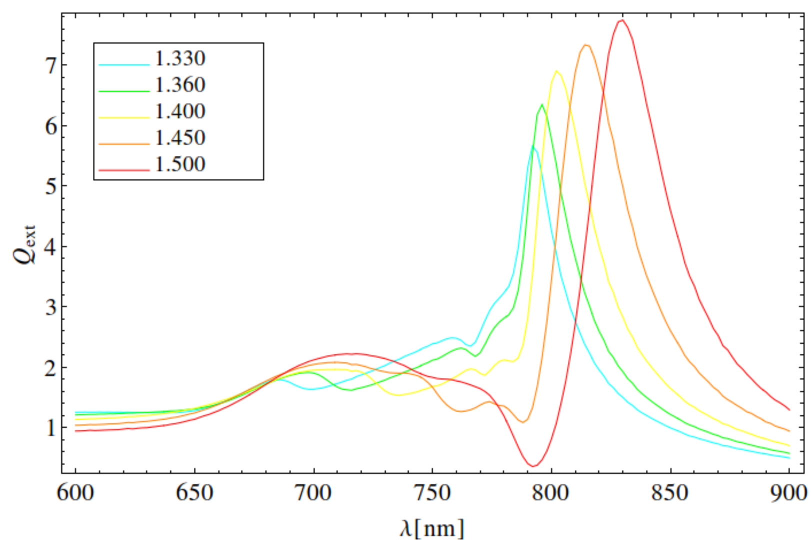

Figure 5: Extinction efficiency for different refractive index values of the surrounding media for the array.

We define the sensitivity of our system as the change in the wavelength of the LSPR per the variation of the refractive index as:

$$S = \frac{\partial \lambda_{LPSR}\left[nm\right]}{\partial n\left[RIU\right]} \tag{3}$$

obtaining a value of sensitivity of 231 nm/RIU. A similar study was then done this time using the phase difference between the two polarization excitations:

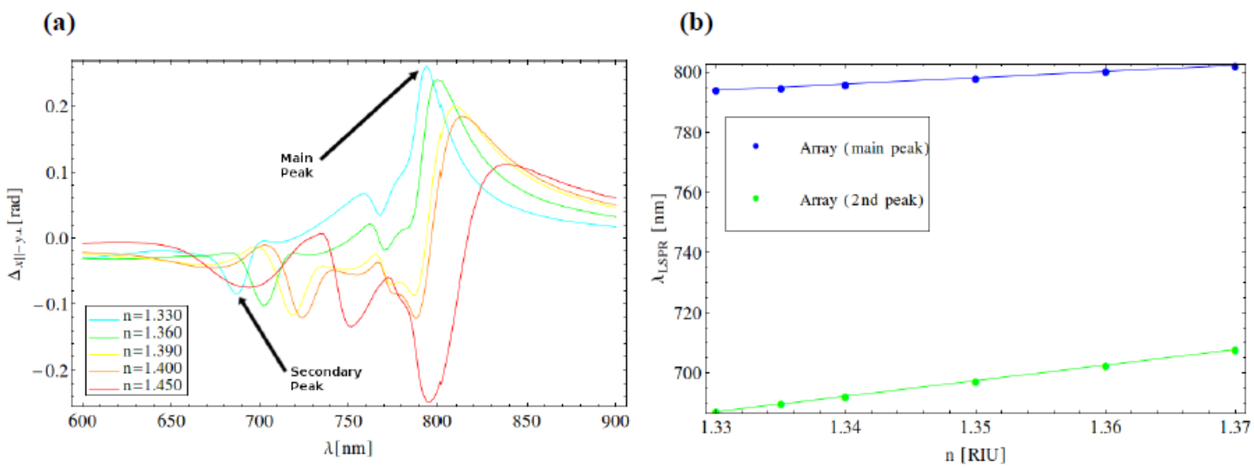

Figure 6: (a) Phase difference spectra for different refractive index values of the surrounding media for the bowtie array. (b) A comparison of phase difference LSPR peak wavelengths for the secondary peak and the main peak.

We define the phase sensitivity as the change in phase retardation over the variation of the refractive index [26]:

$$S_{phase} = \frac{\partial \Delta_{\varphi}\left[rad\right]}{\partial n\left[RIU\right]} \tag{4}$$

and the Detection Limit (DL) can be defined as the resolution (sigma) of the phase measurement system to be used divided by the phase sensitivity of our nanostructure [Equation 4]:

$$DL = \frac{\sigma\left[rad\right]}{S_{phase}\left[rad/RIU\right]} \tag{5}$$

The resolution of the setup to be used was determined from multiple measurements of a quartz sample with a known birefringence at 10^{-7} rad [27].
The best phase sensitivity obtained was 4.75 rad/RIU at a wavelength of 790 nm, which is not surprising given the sharp profile of the LSPR features in Fig. 6a.

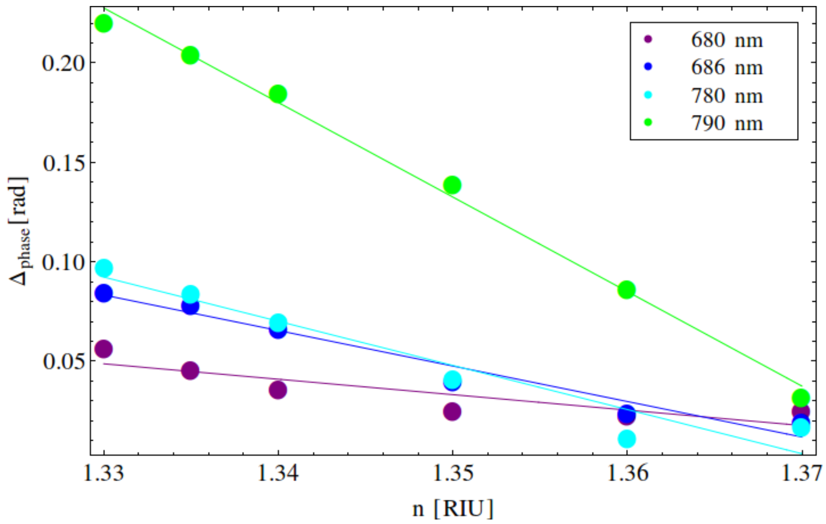

Figure 7: Phase sensitivity fits at different wavelengths for the bowtie array

Although the redshift rate of the secondary LSPR peak is far greater than that of the main peak, the main peak is narrower and therefore can provide a lower detection limit below 10^{-7} RIU.

3.2.2 Surface sensing

For many bioassays the analyte capture would take place within the first 10-20 nm from the surface of the nanoantennas, where the electromagnetic field is enhanced, an so the surface sensitivity of the nanoantennas array was studied by simulating a coverage of 5 nm thick bioreceptor and analyte layers on them under parallel and perpendicular polarization. The first layer, the bioreceptor, was defined by a constant refractive index of 1.39, which is a suitable value for a protein layer [28], and the second, the analyte, was chosen as a variable refractive index in order to simulate various surface concentrations. The biomolecular coating leads to the redshift of the resonance wavelength.

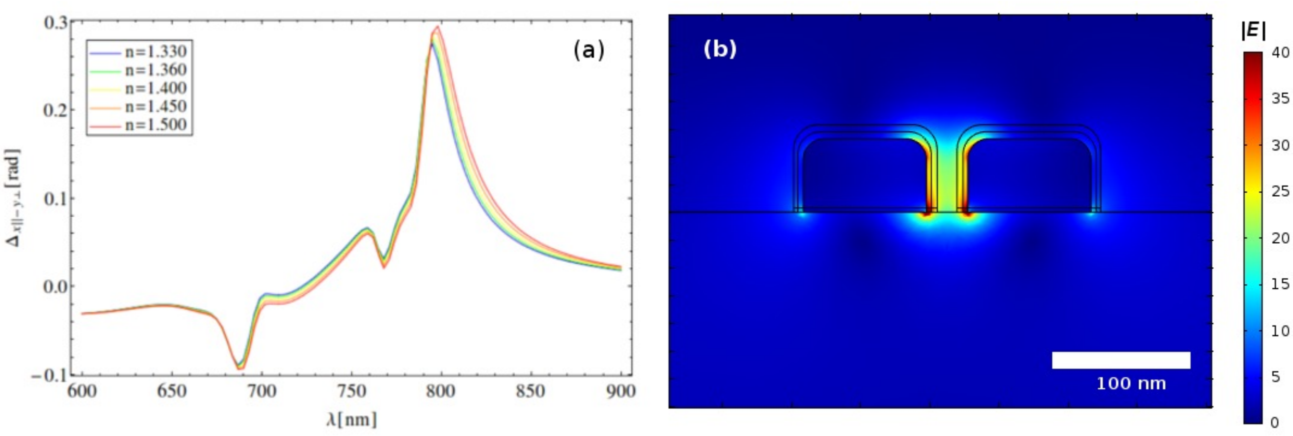

Figure 8: (a) Phase difference spectra of the covered bowtie array for different refractive indexes of the outer biomolecular layer, (b) Distribution of the electric field surrounding the dual biomolecule layer covered nanoantenna for parallel polarization.

The DLs obtained for the phase measurement are less than 10^{-5}, one and two orders of magnitude greater than the volumetric DLs of the single bowtie and array, respectively, which is consistent with other studies of surface detection limits, involving metallic nanogratings for instance [29].

4. CONCLUSIONS

Simulations based on the Finite Element Method were performed to optimize bowtie array designs in order to find the most suitable plasmonic peak for biosensing. From the optimal design, the sensitivity was then determined by simulating the phase retardation for both perpendicular polarizations of the incident plane wave upon varying the refractive index of the surrounding aqueous medium. A similar analysis for surface sensitivity was then performed through the addition of bound layers of bioreceptors and analytes, for a variable analyte RI. Volumetric detection limits below 10^{-7} are obtained for the gold bowtie array based polarimetric sensor comparing them favourably with state of the art plasmonic sensors [30], while surface detection limits were found to be two orders of magnitude higher.

ACKNOWLEDGMENTS

This work was supported through the Generalitat Valenciana and Spanish MINECO under Grants Nos. PROMETEO/2009/074 and TEC2011-29120-C05-01, respectively. Thanks are also given to the FORTEZA program of the Generalitat Valenciana.

REFERENCES

[1] Nahla A. Hatab, Chun-Hway Hsueh, Abigail L. Gaddis, Scott T. Retterer, Jia-Han Li, Gyula Eres, Zhenyu Zhang, and Baohua Gu, *Free-Standing Optical Gold Bowtie Nanoantenna with Variable Gap Size for Enhanced Raman Spectroscopy*, DOI: 10.1021/nl102963g | Nano Lett. 2010, 10, 4952–4955

[2] Brian J. Roxworthy, Kaspar D. Ko, Anil Kumar, Kin Hung Fung, Edmond K. C. Chow, Gang Logan Liu, Nicholas X. Fang, and Kimani C. Toussaint, Jr. , *Application of Plasmonic Bowtie Nanoantenna Arrays for Optical , Trapping, Stacking, and Sorting*, DOI: 10.1021/nl203811q | Nano Lett. 2012, 12, 796−801

[3] Brian J. Roxworthy and Kimani C. Toussaint, Jr., *Plasmonic nanotweezers: strong influence of adhesion layer and nanostructure orientation on trapping performance*, doi: 10.1364/OE.20.009591 | Vol. 20, No. 9 / Optics Express 9591 (2012)

[4] Jeffrey N. Anker, W. Paige Hall, Olga Lyandres, Nilam C. Shah, Jing Zhao and Richard P. Van Duyne, *Biosensing with plasmonic nanosensors*, DOI: 10.1038/nmat2162 | Nature Materials 7, 442 - 453 (2008)

[5] Srdjan S. Acimović, Mark P. Kreuzer, María U. González and Romain Quidant, *Plasmon Near-Field Coupling in Metal Dimers as a Step towards Single-Molecule Sensing*, DOI: 10.1021/nn900102j | AcsNano Vol. 3, No. 5, 1231-1237 (2009)

[6] Arvind Sundaramurthy, K. B. Crozier, G. S. Kino, D. P. Fromm, P. J. Schuck and W. E. Moerner, *Field enhancement and gap-dependent resonance in a system of two opposing tip-to-tip Au nanotriangles*, Physical Review B 72, 165409 (2005)

[7] Ronen Adato, Ahmet Ali Yanik, Chih-Hui Wu, Gennady Shvets and Hatice Altug, *Radiative engineering of plasmon lifetimes in embedded nanoantenna arrays*, 1 March 2010 / Vol. 18, No. 5 / Optics Express 4526

[8] Shengli Zou, Nicolas Janel, and George C. Schatz , *Silver nanoparticle array structures that produce remarkably narrow plasmon lineshapes*, DOI: 10.1063/1.1760740 | J. Chem. Phys. 120, 10871 (2004)

[9] J. Álvarez, C. Serrano, D. Hill, J. Martínez-Pastor, *Real-time polarimetric optical sensor using macroporous alumina membranes*, Optic Letters 38, 7, (2013), pp 1058-1060

[10] Stefania Dante, Daphné Duval, Borja Sepúlveda, Ana Belen González-Guerrero, José Ramón Sendra and Laura M. Lechuga, *All-optical phase modulation for integrated interferometric biosensors*, 26 March 2012 / Vol. 20, No. 7 / Optics Express 7195

[11] Chung-Tien Li, How-foo Chen, Ieng-Wai Un, Hsin-Cheng Lee and Ta-Jen Yen, *Study of optical phase transduction on localized surface plasmon resonance for ultrasensitive detection*, 30 January 2012 / Vol. 20, No. 3 / Optics Express 3251

[12] E. D. Palik, Handbook of Optical Constants of Solids (Academic Press, 1997).

[13] P. J. Schuck, D. P. Fromm, A. Sundaramurthy, G. S. Kino and W. E. Moerner, *Improving the Mismatch between Light and Nanoscale Objects with Gold Bowtie Nanoantennas*, PRL 94, 017402 (2005)

[14] COMSOL MULTIPHYSICS, Comsol Inc. (http://www.comsol.com)

[15] Alexander V. Kildishev, Joshua D. Borneman, Kuo-Ping Chen and Vladimir P. Drachev, *Numerical Modeling of Plasmonic Nanoantennas with Realistic 3D Roughness and Distortion,* DOI: 10.3390/s110707178 | Sensors 2011, 11, 7178-7187

[16] Stephanie Dodson, Mohamed Haggui, Renaud Bachelot, Jérôme Plain, Shuzhou Li and Qihua Xiong, *Optimizing Electromagnetic Hotspots in Plasmonic Bowtie Nanoantennae*, DOI: 10.1021/jz302018x | J. Phys. Chem. Lett. 2013, 4, 496−501

[17] Tzy-Rong Lin, Shu-Wei Chang, Shun Lien Chuang, Zhaoyu Zhang and P. James Schuck, *Coating effect on optical resonance of plasmonic nanobowtie antenna*, Applied Physics Letters 97, 063106 (2010)

[18] Wei Ding, Renaud Bachelot, Sergei Kostcheev, Pascal Royer and Roch Espiau de Lamaestre, *Surface plasmon resonances in silver Bowtie nanoantennas with varied bow angles*, DOI: 10.1063/1.3524504 | Journal of Applied Physics 108, 124314 (2010)

[19] Gang Bi, Li Wang, Li Ling, Yukie Yokota, Yoshiaki Nishijima, Kosei Ueno, Hiroaki Misawa, Jianrong Qiu, *Optical properties of gold nano-bowtie structures*, DOI: 10.1016/j.optcom.2012.12.080 | Optics Communications 294 (2013) 213–217

[20] Hongming Shen, Guowei Lu, Tianyue Zhang, Jie Liu, Ying Gu, Pascal Perriat, Matteo Martini, Olivier Tillement and Qihuang Gong, *Shape effect on a single-nanoparticle based plasmonic nanosensor,* Nanotechnology 24 (2013) 285502

[21] Xiaojin Jiao, Jeremy Goeckeritz, Steve Blair, Mark Oldham, *Localization of Near-Field Resonances in Bowtie Antennae: Influence of Adhesion Layers*, DOI: 10.1007/s11468-008-9075-x | Plasmonics (2009) 4:37–50

[22] Mark W. Knight, Yanpeng Wu, J. Britt Lassiter, Peter Nordlander and Naomi J. Halas , *Substrates Matter: Influence of an Adjacent Dielectric on an Individual Plasmonic Nanoparticle*, DOI: 10.1021/nl900945q | Nano Lett. 9, 5, 2009, 2188-2192

[23] Nathan C Lindquist, Prashant Nagpal, Kevin M McPeak, David J Norris and Sang-Hyun Oh, doi: 10.1088/0034-4885/75/3/036501| Engineering metallic nanostructures for plasmonics and nanophotonics, | Rep. Prog. Phys. 75 (2012) 036501 (61pp)

[24] Daniel Weber, Pablo Albella, Pablo Alonso-González, Frank Neubrech, Han Gui, Tadaaki Nagao, Rainer Hillenbrand, Javier Aizpurua and Annemarie Pucci, *Longitudinal and transverse coupling in infrared gold nanoantenna arrays: long range versus short range interaction regimes*, 1 August 2011 / Vol. 19, No. 16 / Optics Express 15047

[25] Chun-Hway Hsueh, Chih-Hong Lin, Jia-Han Li, Nahla A. Hatab and Baohua Gu, *Resonance modes, cavity field enhancements and long-range collective photonic effects in periodic bowtie nanostructures*, 26 September 2011 / Vol. 19, No. 20 / Optics Express 19660

[26] Jan Becker, Andreas Trügler, Arpad Jakab, Ulrich Hohenester and Carsten Sönnichsen, *The Optimal Aspect Ratio of Gold Nanorods for Plasmonic Bio-sensing*, DOI:10.1007/s11468-010-9130-2 | Plasmonics (2010) 5:161–167

[27] J. Álvarez, N. Kumar, P. Bettotti, D. Hill, J. Martínez-Pastor, *Phase-Sensitive Detection for Optical Sensing With Porous Silicon*, IEEE Photonics Journal, Volume 4, Number 3, 986-995, June 2012

[28]Janos Boros, *The density and refractive index of adsorbing protein layers*, Biophysical Journal Volume 87 July 2004 553-561

[29] Silvio Savoia, Armando Ricciardi, Alessio Crescitelli, Carmine Granata, Emanuela Esposito, Vincenzo Galdi and Andrea Cusano, *Surface sensitivity of Rayleigh anomalies in metallic nanogratings*, DOI:10.1364/OE.21.023531 | 7 October 2013 / Vol. 21, No. 20 / Optics Express 23532

[30] Ian M. White and Xudong Fan, *On the performance quantification of resonant refractive index sensors*, 21 January 2008 / Vol. 16, No. 2 / Optics Express 1021